

# Evaporation of inkjet printed pico-liter droplet on heated substrates with different thermal conductivity<sup>†</sup>

Taewoong Lim, Jaeik Jeong, Jaewon Chung\* and Jin Taek Chung

*Department of Mechanical Engineering, Korea University, Seoul, 136-701, Korea*

(Manuscript Received March 21, 2009; Revised April 2, 2009; Accepted April 2, 2009)

---

## Abstract

In this work, the evaporation phenomena of 20–45 picoliter water droplet (i.e. 50–65  $\mu\text{m}$  diameter) on heated substrates with different thermal conductivity are studied experimentally. The effect of thermal conductivity of substrates and inter-distance between jetted droplets on the evaporation is investigated. In addition, the model to predict evaporation rate of the picoliter droplet on different substrates at a heated condition is developed using approximations for picoliter droplet.

*Keywords:* Droplet; Evaporation; Flexible electronics; Inkjet

---

## 1. Introduction

In typical graphical inkjet printing, the suspended materials are deposited on paper by absorbing the solvent of ink. However, in non-graphical applications, such as the color filter printing, the direct patterning of various functional materials for flexible film as well as printed circuit board, etc., evaporation of solvent results in deposition of suspended materials. Therefore, the understanding of the evaporation phenomena of a picoliter droplet is important. Especially, when multiple droplets are jetted at the same spot to increase the thickness of deposition material maintaining the pattern width as minimum, the next droplet should impact after the most solvent of the previous droplet evaporates [1]. In addition, the evaporation rate is known to affect the coffee ring phenomena.

In this work, the evaporation phenomena of 20–45 picoliter droplet (i.e. 50–65  $\mu\text{m}$  diameter) on the heated substrates with different thermal conductivity are studied experimentally. Based on the previous

model to predict evaporation rate of the picoliter droplet [1] on the highly conductive substrate, the model considering the effect of thermal conductivity of substrates is developed and the validity of the approximation used in the model is discussed.

## 2. Experimental setup

The drop-on-demand (DOD) printing system used in the experiment is shown in Fig. 1 [1, 2]. Briefly, MicroFab's piezo-jet heads with 30 $\mu\text{m}$  of nozzle diameters are driven by the amplified bipolar voltage waveform (about  $\pm 10\text{--}20\text{V}$ ) with about 40 $\mu\text{s}$  of the dwell time and a picoliter droplet with a few m/s velocity is generated. The jetting frequencies are 5, 10, and 30Hz moving a single nozzle at 2.73mm/s, so that the center to center inter-distance between jetted droplets are 546, 273, and 91  $\mu\text{m}$ , respectively. The temperature of the substrate is controlled within 2°C by thermocouple and the Mica heater in the vacuum chuck to see the effect of the substrate heating on the droplet evaporation. The sequential images of the evaporating droplet are obtained by high speed camera (IDT, MotionPro X3) using continuous illumination.

---

<sup>†</sup> This paper was presented at the 7th JSME-KSME Thermal and Fluids Engineering Conference, Sapporo, Japan, October 2008.

\*Corresponding author. Tel.: +82 32 872 309682 2 3290 3374, Fax.: +82 32 868 171682 2 926 9290

E-mail address: kykim@inha.ac.kr; jw@koreac.ac.kr

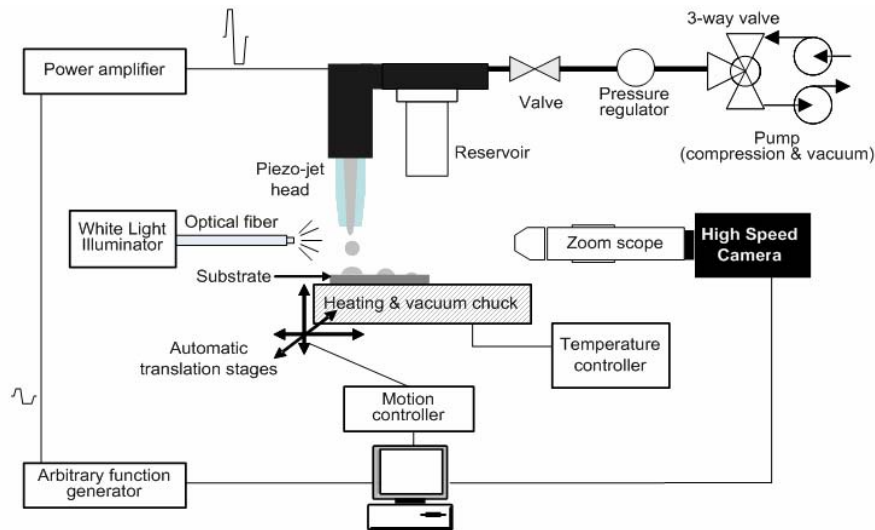


Fig. 1. Schematic of inkjet printing system and droplet.

When the droplet oscillation after impact is damped out after several hundred microseconds [1], both the Bond number and the capillary number are small for the picoliter droplet, so that the sessile droplet has the shape of a spherical cap. Therefore, geometric parameters of the evaporating the sessile droplet, such as droplet height ( $h$ ), contact radius ( $R$ ), radius of curvature ( $r$ ), contact angle ( $\theta$ ), droplet volume ( $V$ ) can be determined by measurement of two parameters using the following relationships.

$$h = \frac{R(1 - \cos \theta)}{\sin \theta} \quad (1)$$

$$V = \frac{\pi}{3} h^2 (3r - h) = \frac{\pi}{3} R^3 \frac{(1 - \cos \theta)(2 + \cos \theta)}{\sin \theta (1 + \cos \theta)} \quad (2)$$

Three geometric parameters of the sessile droplet ( $r$ ,  $R$  and  $h$ ) are measured automatically by using a custom made LabView image processing code (Fig. 2). The original image showing the side view of the sessile droplet has the shape of double spherical caps due to reflection from the substrate surface (e.g. Fig. 2(a) and Fig. 3(b)). First, the edge of the sessile droplet is obtained by eliminating the relatively bright background in step (b) in Fig. 2. Here, the threshold which defines the edge of the sessile droplet is determined manually for different illumination conditions (exposure time of the high speed camera, magnifying power, etc). Then, the noisy dots due to dust particle on the lens or CCD are filtered out in step (c). In step (d), the radius of the curvature is fitted from the inter

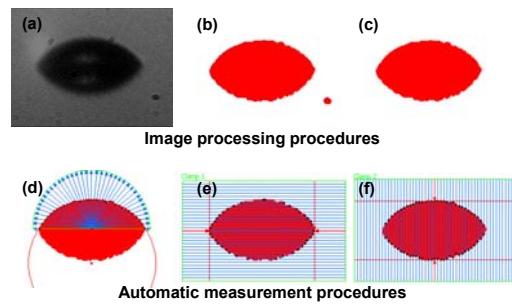


Fig. 2. Image processing and automatic measurement procedures. (a) Original image, (b) Background removal, (c) Noise elimination, (d) Curvature fitting, (e) Contact radius measurement, (d) Height measurement.

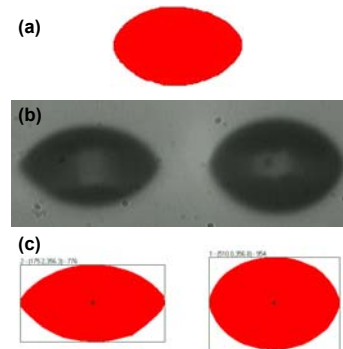


Fig. 3. Measurement of center position (a) Pattern template, (b) Target images, (c) Pattern matching results.

section points between the radial lines from the center and the upper edge of the sessile droplet. Finally, the contact radius and the height of the sessile droplet are

also obtained using the intersection points between the horizontal and vertical lines and the edge of the droplet in step (e) and (f), respectively. Note that the measurement of the radius of curvature in step (d) equires the information about the center position of the sessile droplet, which varies depending on the statistical variation of the droplet impact. The center position is obtained by so called “pattern matching technique” using template droplet pattern made beforehand as shown in Fig. 3(a). The examples of the pattern matching results are shown in Fig. 3(c). Note that this automated measurement not only saves time to analyze many images in every elapsed time, but also eliminates the experimental error caused by the bias of an operator.

### 3. Modeling

When evaporation is dominated by vapor diffusion in air, the vapor density in air for evaporating hemispherical droplet can be expressed as

$$\frac{\partial(r\rho_v)}{\partial t} = D \frac{\partial^2(r\rho_v)}{\partial r^2}, \quad (3)$$

where  $r$ ,  $t$ ,  $\rho_v$  and  $D$  are radial distance, time, vapor density and vapor diffusivity in air, respectively. In the Birdi's approach [3], the transient term in the above governing equation was neglected and using the boundary conditions  $\rho_v = \rho_{v,d}$  at  $r = R$  and  $\rho_v = \rho_{v,\infty}$  as  $r \rightarrow \infty$ , the volume evaporation rate,  $dV/dt$  for a hemispherical droplet on a flat surface was obtained as Eq. (4).

$$\frac{dV}{dt} = 2\pi R^2 \frac{dR}{dt} = 2\pi \frac{\rho_{v,d} - \rho_{v,\infty}}{\rho_f} DR \quad (4)$$

Here, the temperature of droplet is assumed uniform, so that  $\rho_{v,d}$  is the saturated vapor density corresponding to the droplet temperature. When only contact radius decreases while maintaining the shape of hemispherical cap, the total evaporation time  $t_{evap}$  can be obtained by integrating Eq. (4) as [4]

$$t_{evap} = \frac{\rho_f R_i^2}{2D(\rho_{v,s} - \rho_{v,\infty})}. \quad (5)$$

When the contact angle of a sessile droplet is not  $90^\circ$ , the evaporation flux is not uniform along the air-fluid interface, so that the spherical symmetry does

not hold. For example, when the contact angle is less than  $90^\circ$ , the vapor adjacent to the edge of the droplet interface can diffuse into the normal radial direction as well as outside direction, so that evaporation flux is stronger near the edge of the droplet interface. Hu et al. [4] considered the edge effect using finite element method, and obtained the following expression by fitting.

$$\frac{dV}{dt} = 2\pi RD \frac{\rho_{v,s} - \rho_{v,\infty}}{\rho_f} (0.135\theta^2 + 0.65) \quad (6)$$

During the droplet evaporation process, various thermal transports can be coupled [5, 6]. When the solvent evaporates, air-liquid interface of droplet undergoes an evaporative cooling, which decreases the temperature of droplet. Since the top center interface has a longer thermal conduction path from the substrate compared to the contact line area, the temperature at the top center interface is lower. This temperature gradient generates the inward Marangoni flow due to negative surface tension gradient, so that interfacial temperature gradient decreases. Therefore, if either Marangoni time scale or thermal diffusion time scale is much smaller than the evaporation time scale, the temperature field inside droplet can be assumed uniform.

Marangoni time scale,  $t_{Ma}$  can be obtained from the droplet size divided by the Marangoni velocity scale [7].

$$t_{Ma} \approx \frac{R\mu}{(d\sigma/dT)\Delta T} \quad (7)$$

Here,  $\mu$ ,  $d\sigma/dT$  and  $\Delta T$  are viscosity, surface tension gradient and the maximum temperature difference along liquid-vapor interface, respectively. In addition, the thermal diffusion time scale inside droplet,  $t_{cond,f}$  can be approximated as

$$t_{cond,f} \approx \frac{R^2}{\alpha_f}, \quad (8)$$

where  $\alpha_f$  is the thermal diffusivity of water. For water droplet with  $30\mu\text{m}$  radius at a room temperature, the evaporation time scale and the thermal conduction time scale are on the order of  $10^{-1}$  and  $10^{-3}$  seconds, respectively, while the Marangoni time scale is in the order of  $10^{-5}$  seconds for  $1^\circ\text{C}$  of temperature differ-

ence. Therefore, the temperature inside droplet can be assumed uniform during evaporation process. For the same droplet at 100°C, both the evaporation time scale and the thermal conduction time scale are in the order of 10<sup>-3</sup>, while the order of Marangoni time scale is 10<sup>-5</sup> for 1°C of temperature difference. Therefore, the same simplification can be made at a high temperature condition, as well.

The conduction time scale of substrate, *t*<sub>cond,s</sub> conduction time scale can be expressed similar to Eq. (8).

$$t_{cond,s} \approx \frac{R^2}{\alpha_s} \tag{9}$$

Here,  $\alpha_s$  is thermal diffusivity of substrate. For silicon wafer, the conduction time scale of substrate, *t*<sub>cond,s</sub> is in the order of 10<sup>-6</sup> second, which is much smaller than the evaporation time scale. Therefore, the uniform temperature distribution in a substrate as well as in a droplet would be a reasonable approximation. However, for glass substrate, the order of the conduction time scale is 10<sup>-4</sup>, which is comparable to the total evaporation time scale at the high temperature condition. In this situation, the temperature distribution in a substrate should be considered to predict the temperature of the droplet and the evaporation process, as well.

Applying energy balance to the droplet, heat transfer rate over the circular contact area of the droplet, *Q*(*t*,*r*) should equal to the summation of the rate change of sensible heat in the droplet and the rate of the latent heat by evaporation.

$$Q(t,r) = \rho_f V C_p \frac{dT_d}{dt} + \rho_f h_{fg} \frac{dV}{dt} \approx \left( \frac{1}{R_{th,s}} \right) (T_{s,\infty} - T_d) \tag{10}$$

Here,  $\rho_f$ ,  $C_p$  and  $h_{fg}$  are the density, the heat capacity, and the latent heat of water, respectively. In Eq. (10), heat transfer rate is simplified to the temperature difference between the substrate and the droplet divided by the thermal resistance over the circular contact area of substrate, *R*<sub>th,s</sub>. Since the temperature of the droplet, *T*<sub>*d*</sub> initially at a room temperature increases after contacting the substrate at an elevated temperature, *T*<sub>*s,∞*</sub> heat flux at the interface will decrease with time. For simplification, *R*<sub>th,s</sub> is approximated as the steady state thermal resistance over the circular area with the constant temperature condition in a semi-infinite medium,  $(4Rk_s)^{-1}$  [8], where *k*<sub>*s*</sub> is the thermal

conductivity of substrate. Then, combining these expressions results in

$$\frac{dT_d}{dt} \approx \frac{4Rk_s(T_{s,\infty} - T_d) - \rho_f h_{fg} \frac{dV}{dt}}{\rho_f V C_p} \tag{11}$$

Using the above results, the evolution of droplet volume is obtained as following. From the initial droplet temperature and the corresponding fluid properties, the volume of evaporation during a small time interval is obtained using Eq. (6) and the new contact angle is obtained from Eq. (2). When the contact angle reaches the receding contact angle, the new radius is obtained in the same way. Then the new contact droplet temperature is obtained from Eq. (11) and the above procedures are repeated with the new droplet temperature.

### 4. Result

Fig. 4 compares the evolution of contact diameter,

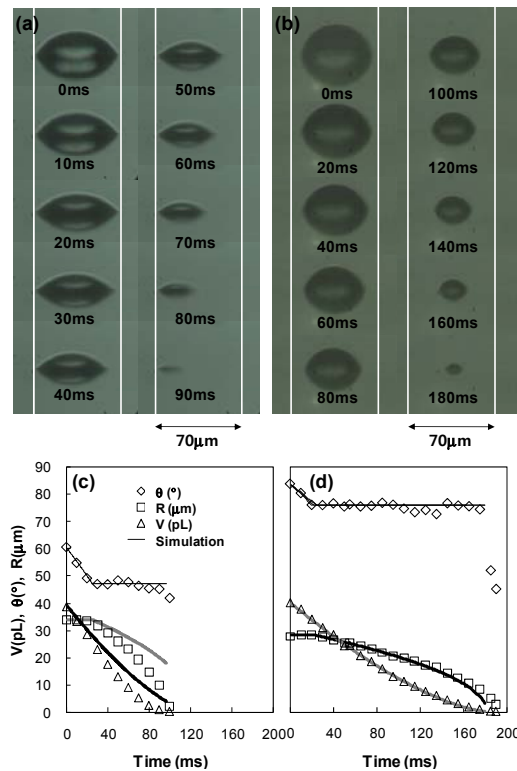


Fig. 4. Temporal evolution of droplet volume, contact angle and contact radius of evaporating water droplet at the jetting frequency of 10Hz (a, c) on the silicon substrate at *T*<sub>*s*</sub>=54°C and (b, d) on the glass substrate at *T*<sub>*s*</sub>=53°C.

contact angle and droplet volume of pure DI water on the silicon substrate and the glass substrate. On the silicon substrate (Fig. 4(a, c)), the contact angle decreases maintaining the constant contact diameter during the initial period. When the contact angle decreases to about 45°, the sessile droplet is depinned and the contact diameter decreases. In the case of the glass substrate (Fig. 4(b, d)), both the initial contact angle and the receding contact angle are higher than

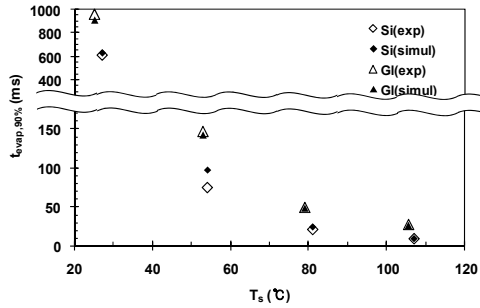


Fig. 5. The evaporation time of water droplet on the silicon substrate ( $V_{init}=38.6\pm 1\text{pL}$ ) and the glass substrate ( $V_{init}=41\pm 1\text{pL}$ ) changing the substrate temperature at the jetting frequency of 10 Hz.

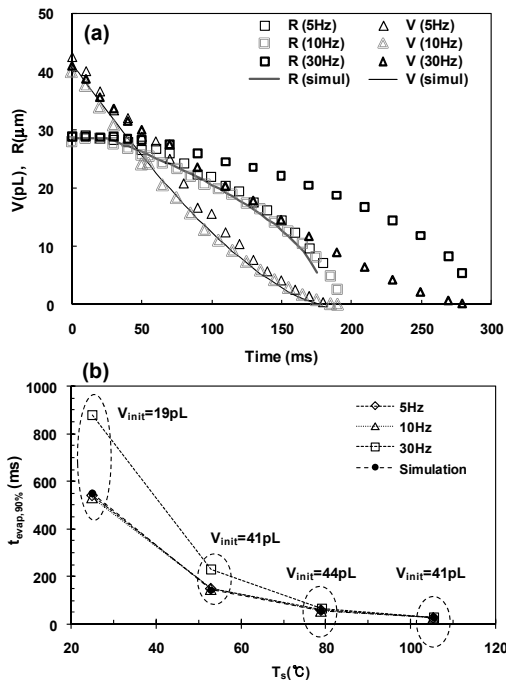


Fig. 6. (a) Temporal evolution of droplet volume, contact angle and contact radius of evaporating water droplet on the glass substrate at  $T_s=53^\circ\text{C}$  changing the jetting frequency, (b) The evaporation time of water droplet on the glass substrate changing the jetting frequency.

the case of the silicon substrate. In addition, the simulation results considering the substrate cooling effect match well with the experimental results.

Fig. 5 shows the time elapsed for evaporating 90% of the initial droplet volume ( $t_{evap,90\%}$ ) with respect to varying temperature of the silicon substrate and glass substrate. The calculated evaporation time (marked by solid symbols) shows good agreement with the experimental results through the entire temperature range.

Fig. 6(a) shows the effect of inter-distance between jetted droplets at the glass substrate temperature of  $53^\circ\text{C}$ . When the jetting frequencies are 5 Hz and 10 Hz (inter-distance are 546 and 273  $\mu\text{m}$ , respectively), both results match well with the simulation result. However, when the jetting frequency is 30 Hz (inter-distance is 91  $\mu\text{m}$ ), the evaporation rate decreases due to the evaporation of neighboring droplets. When the

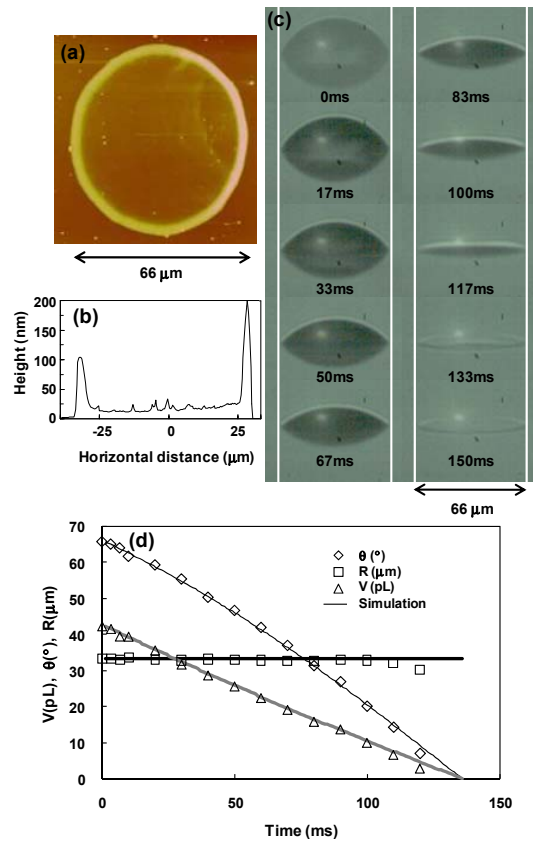


Fig. 7. (a) Atomic force microscope image and (b) the cross-sectional profile of the deposited coffee, (c) time resolved cross-sectional images and (d) temporal evolution of droplet volume, contact angle and contact diameter of water mixed with coffee at  $T_s=53^\circ\text{C}$  at the jetting frequency of 10 Hz on the glass substrate.

substrate temperature is elevated, the evaporation time becomes almost same for all jetting frequencies (Fig. 6(b)).

In real application, the various solutes (i.e. nanoparticles) to be deposited on substrate are often suspended in solvents. Here, to see the effect of solute on the evaporation phenomena, coffee solute is dissolved in water. In this case, the evaporating droplet is pinned during the most of evaporation period due to the deposited coffee at the contact line (Fig. 7(a, b)) and the only contact angle decreases (Fig. 7(c, d)). Even though the macroscopic apparent contact angle becomes smaller than the receding angle of pure water droplet on glass (about  $75^\circ$  in Fig. 4(b, d)), the deposited solute at the contact line makes the microscopic contact angle large. Therefore the pinning can be maintained during the most of evaporation period, which can be often observed in a rough surface. Here, the evaporation period becomes shorter when the solute is dissolved (i.e. from about 190ms in Fig. 4(d) to 130 ms in Fig. 7(d)), since the evaporation area is maintained larger due to pinning. In addition, the vapor diffusion itself is not significantly affected by the solute, so that the calculation results are in good agreement with the experimental results.

## 5. Summary

In this work, the evaporation phenomena of 20–45 picoliter water droplet on heated substrates are studied experimentally. For the glass substrate, the evaporation rate decreases due to a low thermal conductivity compared to the silicon substrate and the vapor diffusion dominated model considering the substrate cooling effect predicts well the experimental results. When the jetting frequency is high (i.e. inter-distance is small), the evaporation rate decreases due to neighboring droplets at the low temperature conditions. When the solute is dissolved, the evaporation

period becomes shorter, since the contact area is pinned during most of evaporation period.

## Acknowledgment

This work was supported by the Korea Research Foundation Grant funded by the Korean Government (MEST) (KRF-2005-041-D00128).

## References

- [1] T. Lim, S. Han, J. Chung, J. T. Chung, S. Ko and C. P. Grigoropoulos, Experimental study on spreading and evaporation of inkjet printed pico-liter droplet on a heated substrate, *Int. J. Heat and Mass Transfer*, 52(1-2) (2009) 431-441.
- [2] J. Chung, S. Ko, C. P. Grigoropoulos, N. R. Bieri, C. Dockendorf and D. Poulikakos, Damage free low temperature pulsed laser printing of gold nanoinks on polymers, *J. Heat Transfer*; 127(7) (2005) 724-732.
- [3] K. S. Birdi, D. T. Vu and A. Winter, A study of the evaporation rates of small water drops placed on a solid-surface, *J. Phys. Chem.*, 93(9) (1989) 3702-3703.
- [4] H. Hu and R. G. Larson, Evaporation of a sessile droplet on a substrate, *J. Phys. Chem. B*, 106(6) (2002) 1334-1344.
- [5] O. E. Ruiz and W. Z. Black, Evaporation of water droplets placed on a heated horizontal surface, *J. Heat Transfer*, 124(5) (2002) 854-863.
- [6] H. Hu and R. G. Larson, Analysis of the effects of Marangoni Stresses on the microflow in an evaporating sessile droplet, *Langmuir*; 21(9) (2005) 3972-3980.
- [7] S. Ostrach, Low-gravity fluid flows, *Annu. Rev. Fluid Mech.*, 14 (1982) 313-345.
- [8] H. S. Carslaw and J. C. Jaeger, *Conduction of heat in solids*, Oxford University Press, New York, USA, (1959).



ing at Hyundai Motor Company.

**Taewoong Lim** received his B.S and M.S. degree in mechanical engineering from Korea University, Seoul, Korea in 2007 and 2009, respectively. His thesis topic was the evaporation of inkjet printed pico-liter droplet and He has been working



**Jaek Jeong** received his B.S. degree in mechanical engineering from Korea University in 2008. He is currently a M.S. candidate in mechanical engineering at Korea University.



was postdoctoral associate in Engineering System

**Jaewon Chung** received his B.S. and M.S. degrees in mechanical engineering from Yonsei University, Seoul, Korea in 1995 and 1997, respectively and Ph.D. degree from University of California, Berkley in 2002. He

Research Center at University of California, Berkley in 2002-2004 and had worked in the Center of Micro and Nano Technology at Lawrence Livermore National Laboratory as a visiting collaborator. He is a currently an associate professor at the Department of Mechanical Engineering at Korea University in Seoul, Korea. His research interests include direct writing methods including drop on demand inkjet printing, electrohydrodynamic printing and laser material processing for printing electronics.



**Jin Taek Chung** received his B.S. and M.S. degrees in mechanical engineering from Korea University, Seoul, Korea in 1983 and 1985, respectively and Ph. D. degree from University of Minnesota, U.S.A. in 1992. He is a currently a professor at the Department of Mechanical Engineering at Korea University in Seoul, Korea. His research interests are heat transfer and 3-D flow in gas turbines and thermal management of electronic devices.